Published in final edited form as:

J Immunol. 2017 October 15; 199(8): 2823–2833. doi:10.4049/jimmunol.1500832.

An anti-inflammatory role for NLRP10 in murine cutaneous leishmaniasis [1]

Gwendolyn M Clay[*,2], **Diogo G Valadares**[‡], **Joel W Graff**[‡,¶,3], **Tyler K Ulland**[*,4], **Richard E Davis**[†], **Breanna M Scorza**[†], **Bayan Sudan Zhanbolat**[‡], **Yani Chen**[‡], **Fayyaz S Sutterwala**[*,†,‡,¶,5], and **Mary E Wilson**[*,†,‡,¶,§,6]

[*]Interdisciplinary Programs in Molecular and Cellular Biology, Iowa City, IA USA

[‡]Department of Internal Medicine, Iowa City, IA USA

[¶]University of Iowa and the Veterans' Affairs Medical Center, Iowa City, IA USA

[†]Immunology, Iowa City, IA USA

[§]Department of Microbiology, Iowa City, IA USA

Abstract

The role of the nucleotide-binding domain and leucine-rich repeat containing receptor NLRP10 in disease is incompletely understood. Using three separate mouse strains lacking the gene encoding NLRP10, only one of which had a coincidental mutation in DOCK8, we documented a role for NLRP10 as a suppressor of the cutaneous inflammatory response to *Leishmania major* infection. There was no evidence the enhanced local inflammation was due to enhanced inflammasome activity. NLRP10/DOCK8 dually deficient mice harbored lower parasite burdens at the cutaneous site of inoculation than wild-type controls, whereas singly NLRP10 deficient had similar parasites loads to controls, suggesting that DOCK8 promotes local growth of parasites in the skin whereas NLRP10 does not. NLRP10-deficient mice developed vigorous adaptive immune responses, indicating there was not a global defect in development of antigen specific cytokine production. Bone marrow chimeras showed the anti-inflammatory role of NLRP10 was mediated by NLRP10 expressed in resident cells in the skin, rather than bone marrow-derived cells. These data suggest a novel role for NLRP10 in the resolution of local inflammatory responses during *L. major* infection.

Keywords

Parasitic-Protozoan; Inflammation; Neutrophils; Transgenic/Knockout Mice; Skin

This work was supported by National Institutes of Health Grants R01 AI045540 (MEW), AI076233 (MEW), AI118719 (FSS), and by Veterans' Affairs Merit Review Grants 5I01BX001983 and 2I01BX000536 (MEW).

[6]Corresponding author: Mary E. Wilson, 319-356-3169, fax 319-384-7208, mary-wilson@uiowa.edu.
[2]Current address: Department of Pediatrics, University of California at San Diego, San Diego, CA. gwen80@gmail.com
[3]Current address: Department of Biological Sciences, Montana Tech University, Butte, Montana. joelgraff@gmail.com
[4]Current address: Department of Pathology and Immunology, Washington University, St. Louis, MO. ullandt@wustl.edu
[5]Current address: Department of Medicine, Cedars-Sinai Medical Center, Los Angeles, CA. fayyaz.sutterwala@cshs.org

Introduction

The nucleotide-binding domain and leucine-rich repeat containing receptor (NLR) family has diverse functions in regulating innate immunity and inflammation. Activation of some NLR proteins, including NLRP1, NLRP3, and NLRC4, triggers assembly of inflammasome complexes, resulting in the activation of caspase-1 which in turn processes pro-IL-1β and pro-IL-18 into their mature secreted forms. However, the majority of NLR proteins have not been shown to mediate inflammasome complex formation. These “non-inflammasome” NLRs have diverse functions in inflammation and immunity that are still being defined. NLRP6, NLRP12, and NLRP10 have all been described as inhibitors of innate immune responses (1–8).

NLRP10 is widely expressed in myeloid cells, epithelial cells, and keratinocytes. It is the only NLR protein without a leucine rich repeat (putative ligand-binding) domain, leading investigators to hypothesize that it acts as a dominant negative inhibitor of inflammasomes. As such, anti-inflammatory properties of NLRP10 have been attributed to inhibition of inflammasome activation via ASC binding and inhibition of ASC-mediated NF-κB activation (6, 8). A contrasting pro-inflammatory role for NLRP10 has also been implicated through a study of *Shigella flexneri* infection, in which NLRP10 contributed to inflammatory cytokine release, possibly by interacting with NOD1 and its down-stream pathway components (9). Although NLRP10 was implicated in adaptive immune responses through the regulation of dendritic cell migration, recent studies revealed a coincident mutation in DOCK8 in NLRP10-deficient mice, and suggested that DOCK8 was responsible for the observed phenotype (10). Thus, the functions of NLRP10 in innate immunity need further investigation.

Leishmaniasis refers to a group of diseases caused by the intracellular *Leishmania* spp. protozoa. Cutaneous leishmaniasis, the most common form of human disease, is defined by inflammatory ulcerative lesions limited to the skin. Studies of mouse models with cutaneous leishmaniasis caused by *Leishmania major* infection revealed dichotomous manifestations in different inbred mouse strains, which fortuitously illustrated differential outcomes of TH1-type versus TH2-type immunity. Susceptible BALB/c mice developed a strong TH2-type response to a dominant *L. major* antigen (LACK) leading to disease progression and parasite visceralization to the liver and spleen. In contrast, resistant mice such as the C57BL/6 line displayed a predominantly TH1-type response leading to disease self-clearance and protective immunity (11, 12). Subsequent studies have revealed that innate immune responses initiated at the onset of infection are critical determinants of the type of adaptive immune response that develops, and the outcome of disease (13–15). As an example, localized events occurring at the onset of infection in resistant mice have been shown to promote the rapid local production of cytokines, including IL-6 and IL-1β, and a subsequent effective adaptive immune response (15). These studies underscore the importance of understanding the roles of innate immune mechanisms in leishmaniasis.

NLRP3 inflammasome activation has been implicated in both resistance and susceptibility in murine models of cutaneous leishmaniasis (16–18). However, the role of other NLRs in leishmaniasis is unknown. We therefore undertook a screen of mouse strains lacking NLR

proteins NLRP6, NLRP12, and NLRP10 in order to document the roles of each of these incompletely understood NLRs in *L. major* infection. Because of its critical role in inflammasome formation, mice lacking the adaptor protein ASC were included as a screen for inflammasome involvement. The course of lesion development and parasite burden in these knockout mice were compared to the self-healing wild type (WT) mice on a C57BL/6 background. Our observations revealed an anti-inflammatory role for NLRP10 in cutaneous leishmaniasis, but not in the local control of parasite growth. Data also suggest that this effect is not due to uncontrolled inflammasome activation, but rather due to a vigorous infiltration/retention of neutrophils at the local site of inflammation. These data suggest an anti-inflammatory effect of NLRP10 is a partial determinant of symptomatic disease during cutaneous leishmaniasis, independent of controlling or promoting growth of the parasite itself.

Materials and Methods

Parasites

An *L. major* strain isolated from a patient who acquired cutaneous leishmaniasis in Iraq (IA0) was transfected with SwaI-linearized pLucCherry to generate a transgenic line that expressed both luciferase and mCherry(19). Parasites were passed through mice to maintain virulence, accomplished by inoculating promastigotes in the hock and isolating a new parasite strain after 4–6 weeks. *L. major* Friedlin strain was kindly provided by Philip Scott, University of Pennsylvania. Parasites were maintained as axenic cultures in Schneider's complete medium (Gibco) supplemented with 10% heat-inactivated FBS, 2 mM L-glutamine, 50 μg/ml gentamicin, and 2% male human urine. Parasites were serially passaged in mice to maintain virulence.

Mice and bone marrow chimeras

Female mice were infected with parasites intradermally at 6–8 weeks of age.. Sex and age matched C57BL/6N (Charles River) or BALB/cJ (Jackson Laboratories) mice were used as controls for gene knockout strains. Mice were maintained in specific-pathogen-free housing. All protocols were approved by Institutional Animal Care and Use Committees at the University of Iowa and at the Iowa City VA Medical Center.

NLRP10$^{-/-}$, ASC$^{-/-}$, NLRP6$^{-/-}$ or NLRP12$^{-/-}$ mice were generated as described (20–23). ASC$^{-/-}$, NLRP6$^{-/-}$, and NLRP12$^{-/-}$ mice were backcrossed 10 generations onto a C57BL/6N background. NLRP10$^{-/-}$ mice on a BALB/cJ background were generated by backcrossing for 9 generations. In the final stages of our study, the C57BL/6 NLRP10$^{-/-}$ knockout strain was found to harbor an unexpected point mutation that caused a premature stop codon in *dock8*, resulting in a complete loss of DOCK8 protein. Therefore, NLRP10$^{-/-}$DOCK8$^{+/+}$ mice were generated by further backcrossing with C57BL/6N mice for 3 generations, and a wild-type *Dock8* allele was confirmed by sequence analysis (10). When referring to NLRP10$^{-/-}$ mice, we will refer the first strain generated, i.e. the strain with mutant *dock8* unless otherwise stated.

Bone marrow chimeras were generated by lethally irradiating recipient mice, harvesting donor mouse bone marrow from femurs and retro-orbitally injecting recipient mice with 3×10^6 cells in PBS. Recipient mice recovered for four weeks while on antibiotics and engraftment was confirmed to be greater than 95% in the peripheral blood by flow cytometry using CD45.2 (NLRP10$^{-/-}$) and CD45.1 (WT) markers.

L. major infections and in vivo imaging (IVIS)

Stationary or metacyclic promastigotes suspended in 10 μl of PBS were inoculated intradermally into the right ear. Metacyclic promastigotes were isolated from stationary phase cultures as described (24). Lesions in *L. major* infected mice were monitored by caliper measurement and photography at the indicated times and compared to contralateral uninfected ear. Parasite burden in luciferase-expressing parasite infected mice were quantified by *in vivo* imaging using the IVIS 2000 system (Xenogen). Data were collected as pixels emitted in a consistently sized “region of interest” (ROI). Parasites were quantified from total DNA isolated from tissue homogenates using the DNeasy Blood & Tissue Kit (Qiagen)using qPCR for *Leishmania* kinetoplastid DNA with primers and probes as previously described (25).

Histopathology

Ears were harvested from NLRP10$^{-/-}$ or WT mice at the indicated times after intradermal inoculation of PBS or *L. major* promastigotes. Three micron tissue sections obtained from formalin-fixed tissues embedded in paraffin blocks were stained using hematoxylin and eosin (H&E). Infiltrating leukocytes, including myeloid cell types were quantified using light microscopy with conditions blinded to the observer. The site of infiltration was determined on low magnification, and cells in a minimum of three high power fields (HPFs) per ear within the lesion were quantified for each experimental condition in each experiment. Considering the three replicate experiments, at least 10–15 HPFs total were examined per condition per time point. Leukocytes were identified by morphology, and amastigotes were identified by size, morphology, and the presence of nuclear and kinetoplast DNA.

Cytokine assays

Single cell suspensions were generated from draining retromaxillary lymph nodes or spleens from *L. major* infected or control mice by passage through a sterile 70 μM screen. Red blood cells in splenic preparations were lysed by hypotonic shock. The cells were then seeded at 2×10^5 cells/well in 200 μl of RP10 [RPMI 1640 (Gibco), 10% heat-inactivated FBS (Gibco), 2 mM L-glutamine, 50 μg/ml gentamicin, in round bottomed 96-well plates with or without stimuli. The stimuli included media control, 10 μg/ml total *Leishmania* lysate, live *L. major* parasites at 3:1 parasite: host cell ratio, or wells coated with anti-CD3e antibody at 500 ng/mL overnight. After incubation at 37°, 5% CO_2 for 72 hours, supernatants were collected for cytokine assays. The murine cytokines IFN-γ, IL-1β, IL-4, IL-12p70, IL-6, IL-17A, TNFα, and IL-10 were analyzed in cell supernatants by a Multiplex Luminex Assay (Life Technologies) or Bio-Plex Multiplex Assay (Millipore). IL-17A was detected in whole ear lysates by ELISA using the mouse IL-17A DuoSet ELISA kit from R&D. IL-1β was

detected in by ELISA using monoclonal coating and detection antibodies MAB401 and BAF401, respectively, from R&D.

Flow cytometry

Ear tissues were incubated with Liberase TL (Roche) for two hours at 37°C. Cells were dissociated from fibrous tissue through a 70 μm screen as described (14). Lymph nodes and spleen cells harvested as described above, were stained for viability and surface antigens, and fixed. Primary anti-mouse antibodies for flow cytometry were CD11b, APC/Cy7; Ly6C, FITC; Ly6G, PerCP/Cy5.5; CD11c, biotin and Brilliant Violet 605 from BioLegend and anti-mouse MHCII, CD90.2 (53-2.1), anti CD8 (53-6.7), anti CD4 (RM4-5) from eBioscience. Intracellular stains included anti-mouse IFN-g PE-Cy7 (XMG-1.2, eBioscience), anti-IL-17A (TC11-18H10.1, Biolegend), anti-TNF (MP6-XT22 Biolegend) and anti-IL-10 (JES5-16E3, Biolegend). Live cells were identified using a Zombie Yellow Fixable Viability Kit (Bio Legend). Infiltrating leukocytes were identified by CD11b expression. Neutrophils (PMNs) were identified as $CD11b^{+}Ly6G^{+}$, and inflammatory monocytes (monocytes) as $CD11b^{+}CD11c^{-}Ly6G^{-}Ly6C^{+}$ (26). Lymph node cells for intracellular stain were incubated in 0.1 μg/ml PMA, 1 μg/ml ionomycin and 2 μg/ml brefeldin A for 6 hours. Cells were surface stained, then incubated in 0.5% saponin and stained for intracellular cytokines.

Fluorescence minus one (FMO) controls were used to set all gates (27). Cells were analyzed on a BD LSRII flow cytometer (BD Biosciences) and the results were evaluated using FlowJo software (Tree Star).

Isolation of macrophages, neutrophils, and dendritic cells

Murine bone marrow cells were collected from femurs and cultured in RP10 with 10% L929 supernatant for 7–9 days to obtain bone marrow-derived macrophages (BMDMs). Bone marrow-derived dendritic cells (BMDCs) were generated from bone marrow cells cultured in RP10 supplemented with GM-CSF (50 ng/ml; PeproTech) and IL-4 (20 ng/ml; PeproTech) for 6 days. Bone marrow neutrophils (PMNs) and monocytes were suspended in RP10 following isolation via Percoll step gradients (52%, 69%, and 78%) (GE Healthcare) (28, 29).

In vitro study of inflammasome activation

BMDMs were primed by incubation in 10 ng/mL of LPS (LPS-EB ultrapure, InvivoGen) for 3 hours. Cultures were rinsed and stimulated for 16 hours with 100 μg/mL alum (ImJect alum., Thermo Scientific) for 18 hours. Supernatants were collected and IL1-β was assayed using by ELISA.

In vitro infections of BMDM and BMDC

Metacyclic promastigotes were isolated by density gradient from stationary culture of *L. major* Friedlin strain as previously described and opsonized with 5% A/J (C5a deficient) murine serum (Jackson Laboratories) at 37°C for 15 minutes (24). The parasites were added at a ratio of 5:1 to WT or $NLRP10^{-/-}$ BMDM and BMDCs in wells containing cover slips. After one hour at 35°C, 5% CO_2, cells were washed to remove unbound parasites. The cover

slips were removed at the indicated time points and the parasite-infected BMDM and BMDCs were stained using Hema3 solutions (Fisher Scientific). The percent of cells that were infected, the number of parasites per infected cell, and the total parasites/100 cells were determined by light microscopy.

Chemotaxis assays

In vitro chemotaxis assays were performed with PMNs, mononuclear cells, or BMDCs using a 96-well ChemoTx System (Neuroprobe) with 3 μm, 5 μm, or 8 μm pores sizes respectively. PMN and monocyte chemoattractants were zymosan activated serum [1 mg Zymosan A from *Saccharomyces cerevisiae* (Sigma) per 1 ml autologous serum diluted to 0.5%], MCP-1 (500 or 700 ng/ml; PeproTech), or heat-killed *S. aureus* (10% v/v of overnight culture). BMDC chemoattractants were CXCL12, CCL19, and CCL21 (each at 100 ng/ml; PeproTech). All were diluted in HBSS, and optimal concentrations for chemotaxis assays were determined empirically. Chemoattractants were loaded in triplicate in the lower chambers, and cell suspensions in the upper chambers. After incubation for one hour (for PMNs and monocytes) or two hours (for DCs) at 37°C and 5% CO_2, the upper chambers were removed and cells in the lower chamber were stained with calcein AM for 15 minutes and fluorescence was quantified on a plate reader (485 nm excitation, 530 nm emission).

Statistical analysis

Statistical significance was determined using GraphPad Prism software. Multiple groups were compared using one- or two-way ANOVA with Bonferroni or Tukey post-test. Two group comparisons were performed using Student's t-test, or Wilcoxon Rank Sum for non-parametric data.

Results

NLRP10-deficient mice have increased inflammatory responses to L. major infection, compared to wild-type controls

To determine whether ASC, NLRP6, NLRP10, or NLRP12 play a role in cutaneous leishmaniasis *in vivo* , we inoculated luciferase-expressing *L. major* intradermally into the ears of ASC$^{-/-}$, NLRP6$^{-/-}$, NLRP12$^{-/-}$, or NLRP10$^{-/-}$ mice, all on a C57BL/6 background, and compared lesion development and parasite burden to wild-type (WT) C57BL/6 mice. Parasite burdens were measured according to luciferase activity (photons/second). The same isolate passage was used to infect knockout and control lines in each experiment, allowing us to compare photons emitted between groups within each experiment. Although luciferase activity is proportional to parasite burden within each experiment, it cannot be directly extrapolated to quantify parasite numbers.

As expected, WT C57BL/6 mice exhibited a self-healing phenotype. There were no significant differences between WT mice and mice deficient in ASC, NLRP6, or NLRP12 based upon either lesion size or parasite burden (Figure 1A-C). However, comparison of NLRP10$^{-/-}$ and WT mice infected with luciferase-expressing *L. major* revealed that NLRP10$^{-/-}$ mice developed dramatically larger lesions than infected WT mice, with more frequent ulceration. WT mice resolved their lesions by measures of both size and ulceration,

whereas NLRP10$^{-/-}$ lesions failed to resolve (Figure 1D, F). Surprisingly, this line of NLRP10$^{-/-}$ mice harbored lower parasite burdens than WT mice during the first 8 weeks of infection, although they failed to decrease the parasite burden from initial levels, resulting in higher parasite loads than those observed in WT mice at 14 weeks of infection (Figure 1E). Additional studies revealed these mice had a coincident defect in DOCK8 (30), an observation we investigate below.

Differences in the inflammatory response were evident upon infection with a higher dose of metacyclic luciferase-expressing parasites 14 days post infection. NLRP10$^{-/-}$ mice infected with non-transgenic *L. major* Friedlin strain also had increased lesion size and ulceration during infection, indicating this was not a phenomenon of parasite strain or the presence of the transgene (Supplemental figure 1A).

Because the NLRP10$^{-/-}$ strain was recently reported to contain a coincidental mutation in *Dock8* (confirmed in our NLRP10$^{-/-}$ line) (10), we repeated the infection using a line of our NLRP10$^{-/-}$ mice that had been back-crossed on a C57BL/6 background to restore the wild-type *dock8* alleles (Figure 2A-C). Infection of these NLRP10$^{-/-}$ DOCK8$^{+/+}$ mice with *L. major* non-transgenic Friedlin strain reproduced the pattern of increased inflammation and ulceration that we observed in the NLRP10$^{-/-}$ strain with a mutation in *dock8* . However the parasite loads, measured by either qPCR (Figure 2C) or luciferase activity (not shown), were the same in WT versus the NLRP10$^{-/-}$ DOCK8$^{+/+}$ mouse. These data suggest that NLRP10 is responsible for suppressing the inflammatory response that we observed in the original NLRP10$^{-/-}$ mice, and raise the hypothesis that DOCK8 is responsible for enhancing the parasite load locally in the skin. The nature of enhanced inflammation in draining lymph nodes was primarily myeloid, with increase due to CD11b+ myeloid cells, as well as enhanced infiltrating neutrophils (L6G+) and Ly6C+ monocytes (Figure 2D-F).

NLRP10 has been reported to inhibit inflammasome activation, a hypothesis that seems logical because of the lack of a leucine rich ligand-binding domain (31). However, the response of bone marrow derived macrophages isolated from NLRP10$^{-/-}$ or from WT mice had an indistinguishable release of IL-1β in response to LPS and alum, signals that activate the NLRP3 inflammasome (32) (Figure 2G). Furthermore, the abundance of IL-1β in supernatants of draining lymph node cells from either mouse strain was the same, either in the presence or the absence of soluble parasite antigen (Figure 2H). These data suggest the mechanism through which NLRP10 suppresses inflammatory responses is not by inhibition of inflammasome activation, either in vivo or in cultured macrophages.

NLRP10$^{-/-}$ mice on a BALB/cJ background, a strain that also has a wild-type *Dock8* allele, were infected with luciferase-expressing *L. major* . These mice also showed increased lesion size and accelerated ulceration compared to WT BALB/cJ mice (Figure 3A, C). Similar to the NLRP10$^{-/-}$ Dock8$^{+/+}$ C57BL/6 mice, parasite burden in the ear was not different between WT and NLRP10$^{-/-}$ BALB/c mice (Figure 3B, D). However, there were significantly more disseminated parasites to the draining lymph nodes, livers, and spleens of NLRP10$^{-/-}$ compared to WT BALB/cJ mice (Figure 3E-G). Whether this signifies that different mechanisms of clearance are active in the skin versus visceral organs or whether this result indicates differences in parasite dissemination rates cannot be discerned from the

current data. Similar observations were made upon infection of these mice with non-transgenic *L. major* Friedlin strain (Supplemental figure 1B). As might be predicted, dissemination of *L. major* was not detectable in distal organs of C57BL/6 mice, which are genetically resistant to *L. major* infection (33). Disseminated parasites also could not be detected in NLRP10$^{-/-}$ DOCK8$^{+/+}$ C57BL/6 mice, despite the lack of NLRP10 (data not shown). Together these data show a role for NLRP10 in controlling inflammation locally in infected skin sites.

L. major infected NLRP10$^{-/-}$ mice had increased numbers of infiltrating neutrophils in lesions

To identify the cell types responsible for enlarged lesions in NLRP10$^{-/-}$ mice, we quantified the myeloid cells infiltrating the site of acute *L. major* infection by both microscopy and flow cytometry. Histological examination of infected ear sections revealed the majority of the inflammatory lesion in NLRP10$^{-/-}$ infected tissues was accounted for by a neutrophilic infiltrate. The significant increase in infiltrating neutrophils in NLRP10$^{-/-}$ lesions was evident by 1 week, and continued at 2 weeks post-infection. There were more monocytic cells, but not lymphocytes, two weeks after infection in NLRP10$^{-/-}$ ears than WT ears. Amastigotes were rare, but were detected within monocytic cells at the lesion site and trended higher in WT compared to NLRP10$^{-/-}$ ears (Figure 4A-B).

We confirmed the identity of myeloid cells in the infected ear using flow cytometry (Figure 4C). CD11b+ myeloid cells were identified as monocytes or neutrophils based upon Ly6G, Ly6C and CD11c surface staining. Results of these studies showed that cells isolated from the ear tissue of NLRP10$^{-/-}$ mice had increased myeloid cell numbers when compared to WT mice, and a larger population of PMNs was present in NLRP10$^{-/-}$ compared to WT ears at 14 days post-infection. Draining lymph nodes of the same mice showed significantly higher numbers of neutrophils, and increased resident dendritic cells in NLRP10$^{-/-}$ compared to WT mice (Figure 4D).

At late time points during this chronic infection, the disparity between lesions size in WT and NLRP10$^{-/-}$ ears increased (Figure 1D). Indeed, ear lesions in WT mice had nearly resolved by 98 days of infection (Figure 5A). Histologic examination revealed enhanced cellular infiltrates in NLRP10$^{-/-}$ mouse ears, with significantly more total infiltrating cells and PMNs, but similar numbers of monocytic cells and lymphocytes per HPF compared to WT ears (Figure 5B, C). Furthermore, the majority of the infiltrating cells in the NLRP10$^{-/-}$ ears were PMNs, and the majority of the infiltrating WT cells were monocytic cells (Figure 5B, C).

NLRP10$^{-/-}$ and WT myeloid cells do not differ in chemotaxis or infection with Leishmania

The increase in infiltrating neutrophils in the tissues of infected NLRP10$^{-/-}$ mice could be caused by either an inherently increased or diminished responsiveness of neutrophils to chemoattractants leading to either enhanced infiltration or decreased exit, respectively. Alternatively, local tissues could have enhanced attraction for neutrophils. To examine the first possibility, we examined the rate of migration of WT or NLRP10$^{-/-}$ bone marrow derived neutrophils, monocytes or dendritic cells toward chemoattractants in vitro. Migration

of monocytes toward zymosan activated serum (a source of complement fragment C5a) or MCP-1 (CCL2) did not differ between WT and NLRP10$^{-/-}$ cells (Figure 6A). Migration of PMNs toward zymosan activated serum or heat-killed *S. aureus* did not differ (Figure 6B). The migration of bone marrow-derived dendritic cells toward CXCL12, CCL19 or CCL21 was equally efficient between WT and knockout cells (Figure 6C). This suggests differences between infiltrating myeloid cells in NLRP10$^{-/-}$ versus WT tissues cannot be accounted by inherent differences in migration of these cells in or out of infected tissues. Furthermore, the uptake and the intracellular survival of *L. major* was equivalent in NLRP10$^{-/-}$ and WT macrophages *in vitro* (Figure 6D, E). This suggests that the differences in infection rates were not accounted for by intrinsic defects in myeloid cells.

Despite the lack of differential movement of neutrophils toward chemoattractants noted above, both WT and NLRP10$^{-/-}$ neutrophils increased expression of CXCR-2, ligation of which provides a potent activation signal to neutrophils, upon infection with *L. major* (Figure 7A). Therefore we examined whether chemokines ligating CXCR2, including CXCL-1 and CXCL-2, could be implicated in the different inflammatory responses to *L. major* infection. RT-qPCR assay of ear tissue from infect mice showed there were not differences between the abundance of mRNA encoding either CXCL-1 or CXCL-2 between tissues of WT versus NLRP10$^{-/-}$ mice (Figure 7A).

NLRP10$^{-/-}$ mice mount an enhanced adaptive immune response to L. major

To investigate whether adaptive immune responses to *L. major* infection were modulated by NLRP10-deficiency, we assessed antigen-induced cytokine production in isolated lymphocytes from the draining lymph nodes of 2-week *L. major* infected mice. NLRP10$^{-/-}$ cells produced higher amounts of antigen-specific IFNγ, IL-6, IL-10, and IL-17 compared to WT mice (Figure 8A-D). In contrast, TNF and IL-1β amounts did not differ significantly, and IL-4 production was not detected in supernatants of either WT or NLRP10$^{-/-}$ lymph nodes (Figure 8E, F). According to intracellular flow cytometry, the majority of IFN-γ was derived from CD8+ T cells in both WT and NLRP10$^{-/-}$ lymph nodes, whereas CD4+ T cells were the source of IL-10 and IL-17 (Figure 8G). The total numbers of cytokine producing CD4^{+} or CD8^{+} cells did not differ between NLRP10$^{-/-}$ and WT lymph node cells. IL-17 producing cells extracted from ears were too infrequent to detect significant differences between cytokine producing T cells at the local site of infection in the ear. Nonetheless, there was a two-fold increase in IL-17A detected in the whole ear homogenate from NLRP10-/- mice infected for 2 weeks with *L. major* compared to WT mice (Figure 8H).

Gene expression in infected ears was contrasted between uninfected and infected WT, and infected NLRP10$^{-/-}$ mice (Figure 7A). Infection itself caused a significant increase in expression of *nlrp10, cxcr2*, and *il17a* in infected compared to uninfected tissues of WT mice. The only significant differences between transcripts in tissues of infected NLRP10$^{-/-}$ compared to infected WT mice were absent versus present transcript for NLRP10 (as expected), and a significant increase in expression of IL-17a in tissues of wild type mice. Notably there were no differences between the levels of CXCL1, CXCL2 or CXCR1 between WT and NLRP10$^{-/-}$ ear tissues. CCL3, a chemokine that can be released by neutrophils and attracts monocytes, was also unchanged between the groups. Thus the

differential inflammatory responses could not be attributed to chemokines, although there were greater amounts of both *il17* mRNA and IL-17 protein in the ears of NLRP10$^{-/-}$ compared to WT mice infected with *L. major* .

To address the hypothesis that IL-17 is responsible for increased neutrophil recruitment and enhanced local inflammation, we administered neutralizing anti-IL-17 or isotype control antibody to WT or NLRP10$^{-/-}$ mice immediately prior, and through the first 4 weeks of infection (Figure 7B). The results are shown as the ear thickness after 2 weeks, or lesion volume after 4 weeks when lesion dimensions were evident. At the early time point a significant difference was noted in NLRP10$^{-/-}$ mice treated with neutralizing anti-IL17 compared to isotype controls, allowing ear thickness to remain at the size of WT mice treated with either antibody, as one would expect if IL-17 were responsible for the enhanced inflammation phenotype. However after 4 weeks, WT mice treated with anti-IL17 also had significantly smaller lesions than WT mice treated with isotype suggesting a role for IL17 in promoting inflammatory lesions in both WT and knockout mice. The data suggest a role for IL-17 in the exacerbated phenotype of NLRP10$^{-/-}$ mice, but they do not point to IL-17 as the sole explanation of enhanced inflammation.

NLRP10 functions in a non-hematopoietic compartment

The above data do not definitively localize differences between the inflammatory responses between NLRP10$^{-/-}$ and WT mice to a particular cellular compartment. Given the widely distributed expression of NLRP10 in hematopoietic and non-hematopoietic cells, including epidermal cells and dermal fibroblasts in the skin, we used bone marrow chimeras to query which cell compartment was responsible for the effects of NLRP10 on inflammation and parasite expansion (6, 8). Irradiated NLRP10$^{-/-}$ mice reconstituted with either WT or NLRP10$^{-/-}$ bone marrow exhibited a significantly larger inflammatory lesions, reflected by ear thickness, and tissue damage illustrated by ulceration, than irradiated WT mice receiving either type of bone marrow cells (Figure 9). This suggests that NLRP10 in radio-resistant resident cells is essential for controlling inflammation at the site of infection. Thus, NLRP10 expression in the radiation resistant cells resident in tissues controls inflammation and limits lesion size and ulceration during *L. major* infection.

Discussion

Although the effects of adaptive immune responses in cutaneous leishmaniasis are well documented, critical determinants of immune response and disease manifestations are still being discovered. In the current study we examined the roles of NLR proteins, and specifically the non-inflammasome forming protein NLRP10, in the pathogenesis of *L. major* infection. Study of gene knockout mice revealed a novel and dramatic role for NLRP10 as a modifier of the local inflammatory response. Infected NLRP10$^{-/-}$ mice developed and maintained large inflammatory lesions at the site of *L. major* infection, much of which was accounted for by neutrophils. The enhanced inflammation was observed in three strains of mice lacking NLRP10$^{-/-}$, only one of which had a coincidental defect in DOCK8. We observed no intrinsic differences in microbicidal activity of NLRP10-deficient macrophages to explain the enhanced pathology. Although blunted adaptive T cell responses

in recently published observations of NLRP10$^{-/-}$ model has been associated with a failure of dendritic cell migration (23) was due to a coincidental absence of DOCK8, our observations were not accounted for by a failure to mount antigen-specific adaptive immune responses, since our experiments with these NLRP10$^{-/-}$ mice harboring the *Dock8* mutation developed vigorous Th1-type and Th17-type responses *in vivo* (10). Study of bone marrow chimeric mice reveal that the dramatic local inflammatory response in NLRP10$^{-/-}$ mice was due to the absence of NLRP10 in non-bone marrow derived cells, since tissue damage could not be reversed by adoptive transfer of WT bone marrow into irradiated NLRP10$^{-/-}$ mice.

The enhanced inflammatory infiltrate during *L. major* infection occurred not only in the original NLRP10$^{-/-}$ model in which DOCK8 is also not expressed, but also in back-crossed NLRP10$^{-/-}$ mice on a C57BL/6 background in which the DOCK8 gene was intact, as well as in NLRP10$^{-/-}$ mice on a BALB/c background. Nonetheless other differences between these 3 models were informative. The similarity between inflammatory responses between the mouse strains suggested attenuation of the local inflammatory response can be attributed to NLRP10. However the curious progression of parasite loads in the original NLRP10$^{-/-}$ DOCK8$^{-/-}$ strain seen in Figure 1E was not observed in other models, suggesting the lack of initial local growth but higher parasite load in long term infection might be due to the lack of DOCK8. Interestingly, mice lacking NLRP10 on a BALB/c background exhibited similar parasite loads at the local infection site but increased loads at distal sites. These differences may indicate that cells expressing DOCK8 allow parasite growth locally, whereas systemic spread of the parasite is influenced by NLRP10.

Investigation of potential neutrophil chemoattractants revealed significant differences between the amount of IL-17 mRNA and protein in the tissues of infected NLRP10$^{-/-}$ mice compared to WT. However we did not find differential abundance of other the neutrophil chemoattractants such as the chemokine CXCL1 or its receptors CXCR2 and CXCR1 (34), Neutralizing studies suggested that IL-17 may be a factor promoting inflammatory cell influx in both WT and NLRP10$^{-/-}$ mice, however at present we cannot attribute the enhanced inflammatory phenotype in NLRP10$^{-/-}$ mice solely to IL-17.

The dual roles NLRP10 appears to play in murine cutaneous *L. major* infection may contribute to resolving discrepancies in the literature. NLRP10 may have tissue specific roles, particularly since expression of NLRP10 can vary widely from tissue to tissue. Our finding of an anti-inflammatory function of NLRP10 expressed in skin tissue cells as opposed to bone marrow-derived cells may be related to the high expression of NLRP10 in the dermis and epidermis, including epithelial cells and keratinocytes (6, 8, 9). This anti-inflammatory function was confirmed in two NLRP10$^{-/-}$ models that are sufficient in DOCK8, pinpointing the anti-inflammatory role to NLRP10 itself. NLRP10 may limit the local inflammatory signaling cascades leading to reduced chemoattraction of leukocytes. Candidate cells producing pro-inflammatory signals are keratinocytes and epidermal cells, both of which contribute to immunity to *L. major* infection in mice (15). Thus, the suppressive function of NLRP10 might explain why the absence of NLRP10 leads to vigorous T cell responses and increased lesion inflammation during *L. major* infection. Further investigation of the interaction of NLRP10 with innate immune signaling pathways in the skin may elucidate the mechanism of its anti-inflammatory function.

Data presented in this report implicate NLRP10 as a suppressor of inflammatory responses, but they do not indicate a role for this protein in controlling or allowing expansion of the parasite load. Whether NLRP10 is also essential for dissemination of the organism to distant sites, and whether NLRP10 in stromal cells, and DOCK8 in hematopoietic cells act in concert to control local parasite growth and dissemination are questions that yet need to be addressed. Indeed, the trafficking of mononuclear leukocytes, which support parasite growth, in and out of lesions is an essential component of disease (35, 36).

It can be argued that disease manifestations in cutaneous leishmaniasis are caused by the inflammatory response to infection and not by the parasite (37). This is particularly well demonstrated in humans with mucocutaneous leishmaniasis, a clinical form in which the destructive inflammatory lesions have very few parasites present. Thus an understanding of the molecular pathway(s) that naturally suppress inflammation (such as NLRP10) could reveal novel mechanisms to suppress disease with or without suppression of parasite expansion. Therapeutically targeting these pathways may lead us to novel approaches to treatment that target the inflammatory disfiguring lesions that accompany cutaneous and mucocutaneous *Leishmania* spp. infections, rather than or in combination with targeting the parasite itself.

Supplementary Material

Refer to Web version on PubMed Central for supplementary material.

Acknowledgments

The authors are grateful to Melissa Kurtz for her invaluable assistance with all aspects of experiments, and to Richard Flavell and Millennium Pharmaceuticals for generously providing knockout mice.

References

1. Anand PK, Malireddi RK, Lukens JR, Vogel P, Bertin J, Lamkanfi M, Kanneganti TD. NLRP6 negatively regulates innate immunity and host defence against bacterial pathogens. Nature. 2012; 488:389–393. [PubMed: 22763455]
2. Allen IC, Wilson JE, Schneider M, Lich JD, Roberts RA, Arthur JC, Woodford RM, Davis BK, Uronis JM, Herfarth HH, Jobin C, Rogers AB, Ting JP. NLRP12 suppresses colon inflammation and tumorigenesis through the negative regulation of noncanonical NF-kappaB signaling. Immunity. 2012; 36:742–754. [PubMed: 22503542]
3. Ye Z, Lich JD, Moore CB, Duncan JA, Williams KL, Ting JP. ATP binding by monarch-1/NLRP12 is critical for its inhibitory function. Molecular and cellular biology. 2008; 28:1841–1850. [PubMed: 18160710]
4. Zaki MH, Man SM, Vogel P, Lamkanfi M, Kanneganti TD. Salmonella exploits NLRP12-dependent innate immune signaling to suppress host defenses during infection. Proc Natl Acad Sci U S A. 2014; 111:385–390. [PubMed: 24347638]
5. Zaki MH, Vogel P, Malireddi RK, Body-Malapel M, Anand PK, Bertin J, Green DR, Lamkanfi M, Kanneganti TD. The NOD-like receptor NLRP12 attenuates colon inflammation and tumorigenesis. Cancer cell. 2011; 20:649–660. [PubMed: 22094258]
6. Imamura R, Wang Y, Kinoshita T, Suzuki M, Noda T, Sagara J, Taniguchi S, Okamoto H, Suda T. Anti-inflammatory activity of PYNOD and its mechanism in humans and mice. J Immunol. 2010; 184:5874–5884. [PubMed: 20393137]

7. Kinoshita T, Wang Y, Hasegawa M, Imamura R, Suda T. PYPAF3, a PYRIN-containing APAF-1-like protein, is a feedback regulator of caspase-1-dependent interleukin-1beta secretion. The Journal of biological chemistry. 2005; 280:21720–21725. [PubMed: 15817483]
8. Wang Y, Hasegawa M, Imamura R, Kinoshita T, Kondo C, Konaka K, Suda T. PYNOD, a novel Apaf-1/CED4-like protein is an inhibitor of ASC and caspase-1. International immunology. 2004; 16:777–786. [PubMed: 15096476]
9. Lautz K, Damm A, Menning M, Wenger J, Adam AC, Zigrino P, Kremmer E, Kufer TA. NLRP10 enhances Shigella-induced pro-inflammatory responses. Cell Microbiol. 2012; 14:1568–1583. [PubMed: 22672233]
10. Krishnaswamy JK, Singh A, Gowthaman U, Wu R, Gorrepati P, Sales Nascimento M, Gallman A, Liu D, Rhebergen AM, Calabro S, Xu L, Ranney P, Srivastava A, Ranson M, Gorham JD, McCaw Z, Kleeberger SR, Heinz LX, Muller AC, Bennett KL, Superti-Furga G, Henao-Mejia J, Sutterwala FS, Williams A, Flavell RA, Eisenbarth SC. Coincidental loss of DOCK8 function in NLRP10-deficient and C3H/HeJ mice results in defective dendritic cell migration. Proc Natl Acad Sci U S A. 2015
11. Julia V, Rassoulzadegan M, Glaichenhaus N. Resistance to Leishmania major induced by tolerance to a single antigen. Science. 1996; 274:421–423. [PubMed: 8832890]
12. Kaye P, Scott P. Leishmaniasis: complexity at the host-pathogen interface. Nat Rev Microbiol. 2011; 9:604–615. [PubMed: 21747391]
13. de Moura TR, Oliveira F, Rodrigues GC, Carneiro MW, Fukutani KF, Novais FO, Miranda JC, Barral-Netto M, Brodskyn C, Barral A, de Oliveira CI. Immunity to Lutzomyia intermedia saliva modulates the inflammatory environment induced by Leishmania braziliensis. PLoS Negl Trop Dis. 2010; 4:e712. [PubMed: 20559550]
14. Woelbing F, Kostka SL, Moelle K, Belkaid Y, Sunderkoetter C, Verbeek S, Waisman A, Nigg AP, Knop J, Udey MC, von Stebut E. Uptake of Leishmania major by dendritic cells is mediated by Fcgamma receptors and facilitates acquisition of protective immunity. J Exp Med. 2006; 203:177–188. [PubMed: 16418399]
15. Ehrchen JM, Roebrock K, Foell D, Nippe N, von Stebut E, Weiss JM, Munck NA, Viemann D, Varga G, Muller-Tidow C, Schuberth HJ, Roth J, Sunderkotter C. Keratinocytes determine Th1 immunity during early experimental leishmaniasis. PLoS Pathog. 2010; 6:e1000871. [PubMed: 20442861]
16. Lima-Junior DS, Costa DL, Carregaro V, Cunha LD, Silva AL, Mineo TW, Gutierrez FR, Bellio M, Bortoluci KR, Flavell RA, Bozza MT, Silva JS, Zamboni DS. Inflammasome-derived IL-1beta production induces nitric oxide-mediated resistance to Leishmania. Nat Med. 2013; 19:909–915. [PubMed: 23749230]
17. Gurung P, Karki R, Vogel P, Watanabe M, Bix M, Lamkanfi M, Kanneganti TD. An NLRP3 inflammasome-triggered Th2-biased adaptive immune response promotes leishmaniasis. The Journal of clinical investigation. 2015
18. Charmoy M, Hurrell BP, Romano A, Lee SH, Ribeiro-Gomes F, Riteau N, Mayer-Barber K, Tacchini-Cottier F, Sacks DL. The Nlrp3 inflammasome, IL-1beta, and neutrophil recruitment are required for susceptibility to a nonhealing strain of Leishmania major in C57BL/6 mice. Eur J Immunol. 2016; 46:897–911. [PubMed: 26689285]
19. Novais FO, Carvalho LP, Graff JW, Beiting DP, Ruthel G, Roos DS, Betts MR, Goldschmidt MH, Wilson ME, de Oliveira CI, Scott P. Cytotoxic T cells mediate pathology and metastasis in cutaneous leishmaniasis. PLoS Pathog. 2013; 9:e1003504. [PubMed: 23874205]
20. Sutterwala FS, Ogura Y, Szczepanik M, Lara-Tejero M, Lichtenberger GS, Grant EP, Bertin J, Coyle AJ, Galan JE, Askenase PW, Flavell RA. Critical role for NALP3/CIAS1/Cryopyrin in innate and adaptive immunity through its regulation of caspase-1. Immunity. 2006; 24:317–327. [PubMed: 16546100]
21. Arthur JC, Lich JD, Ye Z, Allen IC, Gris D, Wilson JE, Schneider M, Roney KE, O'Connor BP, Moore CB, Morrison A, Sutterwala FS, Bertin J, Koller BH, Liu Z, Ting JP. Cutting edge: NLRP12 controls dendritic and myeloid cell migration to affect contact hypersensitivity. J Immunol. 2010; 185:4515–4519. [PubMed: 20861349]

22. Elinav E, Strowig T, Kau AL, Henao-Mejia J, Thaiss CA, Booth CJ, Peaper DR, Bertin J, Eisenbarth SC, Gordon JI, Flavell RA. NLRP6 inflammasome regulates colonic microbial ecology and risk for colitis. Cell. 2011; 145:745–757. [PubMed: 21565393]

23. Eisenbarth SC, Williams A, Colegio OR, Meng H, Strowig T, Rongvaux A, Henao-Mejia J, Thaiss CA, Joly S, Gonzalez DG, Xu L, Zenewicz LA, Haberman AM, Elinav E, Kleinstein SH, Sutterwala FS, Flavell RA. NLRP10 is a NOD-like receptor essential to initiate adaptive immunity by dendritic cells. Nature. 2012; 484:510–513. [PubMed: 22538615]

24. Yao C, Chen Y, Sudan B, Donelson JE, Wilson ME. Leishmania chagasi: homogenous metacyclic promastigotes isolated by buoyant density are highly virulent in a mouse model. Exp Parasitol. 2008; 118:129–133. [PubMed: 17706646]

25. Weirather JL, Jeronimo SM, Gautam S, Sundar S, Kang M, Kurtz MA, Haque R, Schriefer A, Talhari S, Carvalho EM, Donelson JE, Wilson ME. Serial quantitative PCR assay for detection, species discrimination, and quantification of Leishmania spp. in human samples. J Clin Microbiol. 2011; 49:3892–3904. [PubMed: 22042830]

26. Petritus PM, Manzoni-de-Almeida D, Gimblet C, Gonzalez Lombana C, Scott P. Leishmania mexicana induces limited recruitment and activation of monocytes and monocyte-derived dendritic cells early during infection. PLoS Negl Trop Dis. 2012; 6:e1858. [PubMed: 23094119]

27. Roederer M. Compensation in flow cytometry. Curr Protoc Cytom. 2002 Chapter 1: Unit 1 14.

28. Boxio R, Bossenmeyer-Pourie C, Steinckwich N, Dournon C, Nusse O. Mouse bone marrow contains large numbers of functionally competent neutrophils. J Leukoc Biol. 2004; 75:604–611. [PubMed: 14694182]

29. Itou T, Collins LV, Thoren FB, Dahlgren C, Karlsson A. Changes in activation states of murine polymorphonuclear leukocytes (PMN) during inflammation: a comparison of bone marrow and peritoneal exudate PMN. Clinical and vaccine immunology : CVI. 2006; 13:575–583. [PubMed: 16682479]

30. Krishnaswamy JK, Singh A, Gowthaman U, Wu R, Gorrepati P, Sales Nascimento M, Gallman A, Liu D, Rhebergen AM, Calabro S, Xu L, Ranney P, Srivastava A, Ranson M, Gorham JD, McCaw Z, Kleeberger SR, Heinz LX, Muller AC, Bennett KL, Superti-Furga G, Henao-Mejia J, Sutterwala FS, Williams A, Flavell RA, Eisenbarth SC. Coincidental loss of DOCK8 function in NLRP10-deficient and C3H/HeJ mice results in defective dendritic cell migration. Proc Natl Acad Sci U S A. 2015; 112:3056–3061. [PubMed: 25713392]

31. Imamura R, Wang Y, Kinoshita T, Suzuki M, Noda T, Sagara J, Taniguchi S, Okamoto H, Suda T. Anti-inflammatory activity of PYNOD and its mechanism in humans and mice. J. Immunol. 2010; 184:5874–5884. [PubMed: 20393137]

32. Tschopp J, Schroder K. NLRP3 inflammasome activation: The convergence of multiple signalling pathways on ROS production? Nat. Rev. Immunol. 2010; 10:210–215. [PubMed: 20168318]

33. Vidal SM, Malo D, Vogan K, Skamene E, Gros P. Natural resistance to infection with intracellular parasites: isolation of a candidate for Bcg. Cell. 1993; 73:469–485. [PubMed: 8490962]

34. Tecchio C, Cassatella MA. Neutrophil-derived chemokines on the road to immunity. Semin Immunol. 2016; 28:119–128. [PubMed: 27151246]

35. Goncalves R, Zhang X, Cohen H, Debrabant A, Mosser DM. Platelet activation attracts a subpopulation of effector monocytes to sites of Leishmania major infection. The Journal of experimental medicine. 2011; 208:1253–1265. [PubMed: 21606505]

36. Saha B, Saini A, Germond R, Perrin PJ, Harlan DM, Davis TA. Susceptibility or resistance to Leishmania infection is dictated by the macrophages evolved under the influence of IL-3 or GM-CSF. Eur J Immunol. 1999; 29:2319–2329. [PubMed: 10427995]

37. Terabe M, Kuramochi T, Ito M, Hatabu T, Sanjoba C, Chang KP, Onodera T, Matsumoto Y. CD4(+) cells are indispensable for ulcer development in murine cutaneous leishmaniasis. Infect Immun. 2000; 68:4574–4577. [PubMed: 10899857]

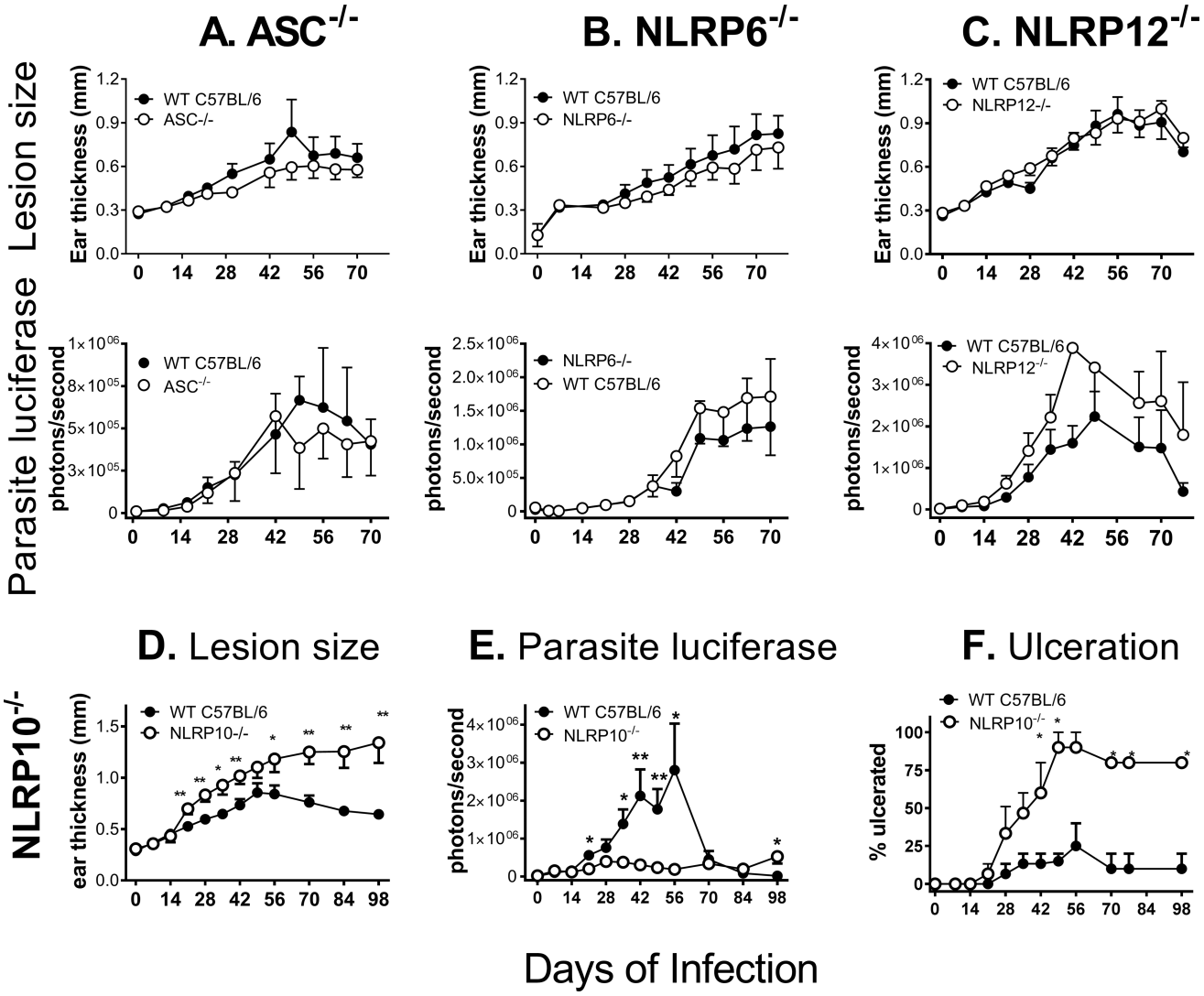

Figure 1. Screens of knockout mouse strains show NLRP10$^{-/-}$ mice, which have a coincident defect on DOCK8, have increased inflammation and lower parasite burdens

WT mice and mice lacking A) ASC, B) NLRP6, C) NLRP12, or D-F) NLRP10, were inoculated intradermally with 5×10^5 luciferase expressing *L. major* stationary promastigotes in the ear pinna. A-E) Lesion development and parasite burden were monitored by weekly caliper measurements of ear thickness and in vivo imaging. F) The percent of NLRP10$^{-/-}$ or control mice in each group with ulcerated lesions was evaluated weekly. Results are pooled data from 3 (A, C-F) or 2 (B) independent experiments. There were 3–9 mice per group in each independent experiment and the results are expressed as the mean ± SEM. (* $p<0.05$; ** $p<0.01$).

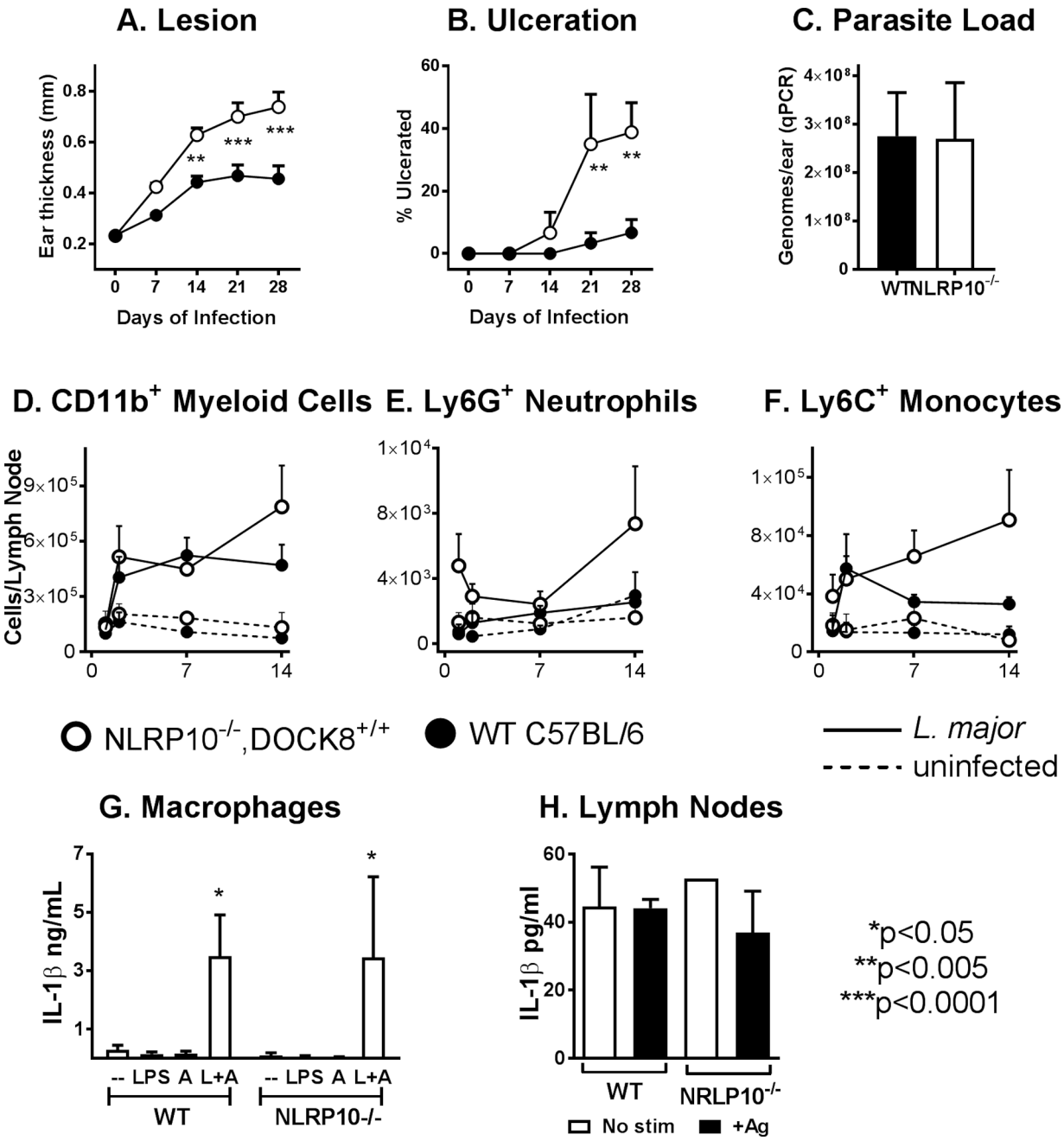

Figure 2. NLRP10$^{-/-}$ DOCK8$^{+/+}$ mice on a C57BL/6 background have enhanced inflammatory responses

(**Panels A-F**): NALP10$^{-/-}$, DOCK8$^{+/+}$ C57BL/6 mice were inoculated with 5×10^5 WT *L. major* metacyclic promastigotes intradermally in the ear pinna. At weekly periods, mice were monitored for (**A**) lesion size by weekly caliper measurement of ear thickness and (**B**) the percentage of mice with ulcerated lesions. (**C**) The parasite burden in total ears was measured in by qPCR after 4 weeks of infection. (Panels **D-F**): WT or NLRP10$^{-/-}$ mice were either infected or inoculated with buffer. After 1, 7 or 14 days, draining lymph nodes were removed from 6–10 mice from each group, stained and evaluated by flow cytometry

for the content of total myeloid cells, neutrophils and infiltrating monocytes. (Panels A-F: n=3 replicate experiments with 6–10 mice per group). (**G-H**): NLRP10 is not required for inflammasome activation in isolated macrophages. G) Inflammasome activation was induced in bone marrow macrophages derived from wild type or NLRP10$^{-/-}$, DOCK8$^{+/+}$ mice by the addition of LPS followed by alum. Mature IL-1β released into supernatants, reflecting inflammasome activation, was measured by ELISA. There were no statistically significant differences between the amounts of IL-1β released after inflammasome activation of wild type C57BL/6 versus NLRP10$^{-/-}$ macrophages (n=5). (**H**) WT or NLRP10$^{-/-}$ mice were infected with *L. major* intradermally in the ear. After 2 weeks, draining lymph nodes lymph nodes were removed and cells were incubated for 48 hrs in buffer (no stim) or *L. major* antigen (+Ag). Supernatants were collected and assessed for IL-1β concentration by ELISA. There were no significant differences between IL-1β released from WT versus NLRP10$^{-/-}$ lymph nodes (2-way ANOVA, n=3).

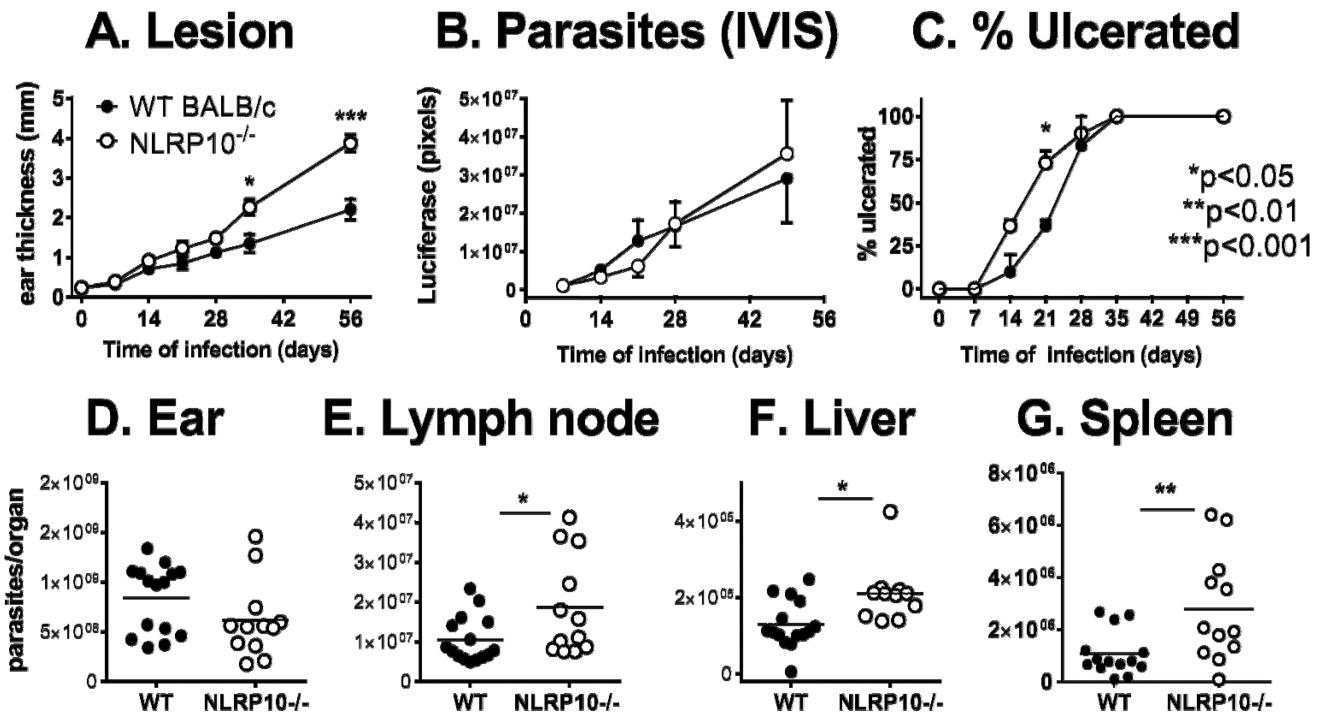

Figure 3. NLRP10$^{-/-}$ mice on a BALB/cJ background have increased lesion size and increased parasites in the visceral organs

Mice were inoculated with 5×10^5 luciferase expressing *L. major* metacyclic promastigotes intradermally in the ear pinna. Panels show (A) Lesion size according to ear thickness measured by calipers, (B) parasite burden according to light generated from luciferase-expressing parasites in the presence of luciferin, and (C) ulceration according to visual inspection, observed for 8 weeks after parasite inoculation. (D-G) Parasite burdens were measured by qPCR in the indicated tissues after euthanizing groups of mice infected for 8 weeks. Results show the mean ± SEM of three independent experiments, each with 3–5 mice per group. Statistical analyses were done by one- or 2-way analysis of variance.

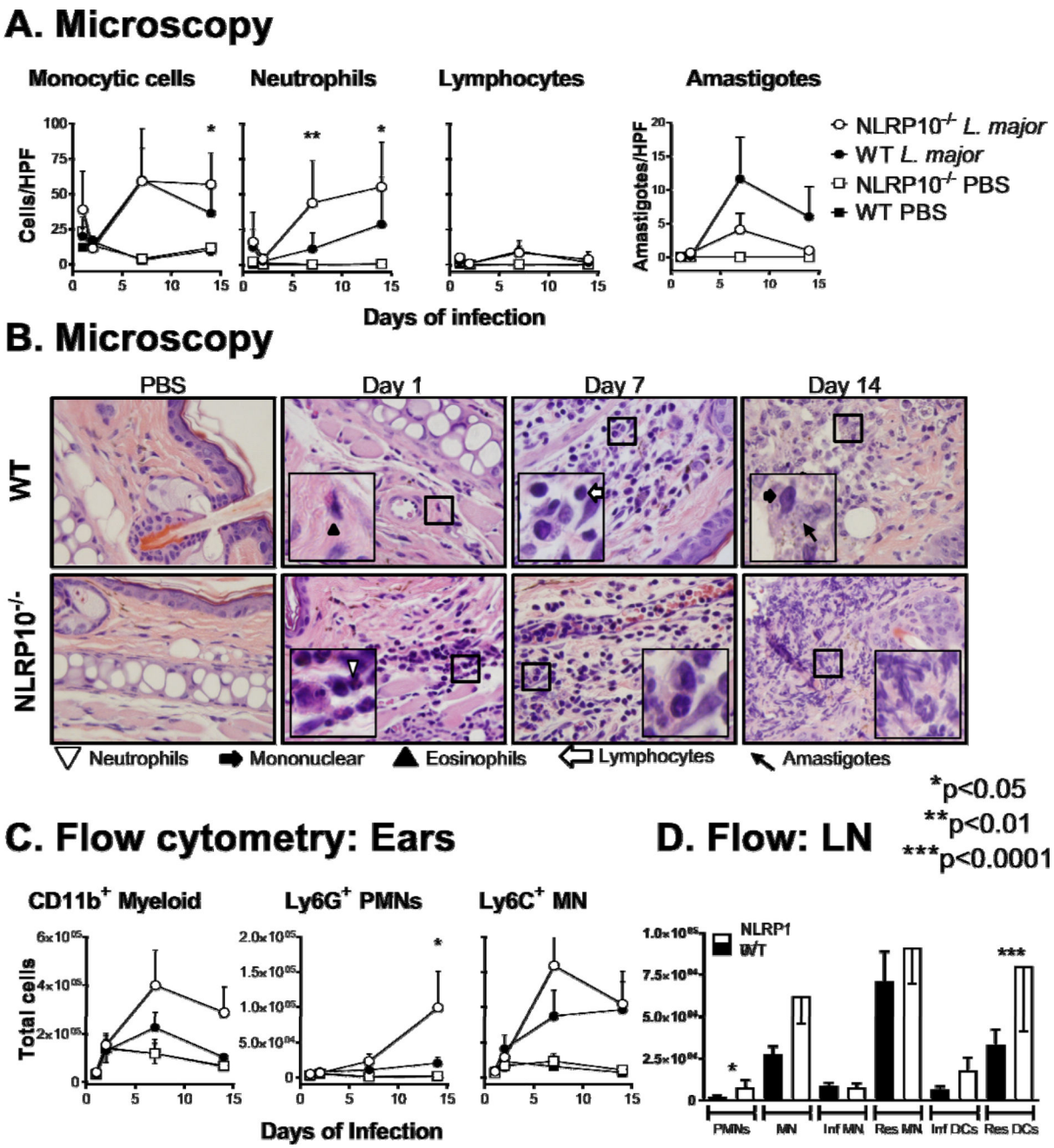

Figure 4. Early lesions: NLRP10$^{-/-}$ mice have more myeloid cell infiltration in acute cutaneous leishmaniasis than WT mice

NLRP10$^{-/-}$ (with coincident DOCK8$^{-/-}$) or WT C57BL/6 mice were inoculated with 1×10^{6} luciferase expressing *L. major* stationary promastigotes intradermally in the ear pinna. (A) The indicated cell types were quantified microscopically in H&E stained histological sections of the ears of mice infected for 1, 2, 7, or 14 days with *L. major* or controls inoculated with PBS at the same time points. Cell numbers are expressed as cells per high power field (HPF) at. (B) Representative images show H&E stained tissue from PBS control or *L. major*- infected ears (100× objective, 1.3 N.A.) with insets illustrating identification of indicated cells. (C) On days 1, 2, 7, and 14 post-infection, cells were isolated from the ears

of 5 mice per group per time point, and analyzed by flow cytometry to quantify the number of the indicated cell types per ear. (D) Draining lymph node cells from the same mice were analyzed by flow cytometry for the indicted cell subsets. Results are compiled from 3 independent experiments, with a minimum of 3 mice per group, and are expressed as the mean ± SEM. Statistical analyses were done by one-way ANOVA.

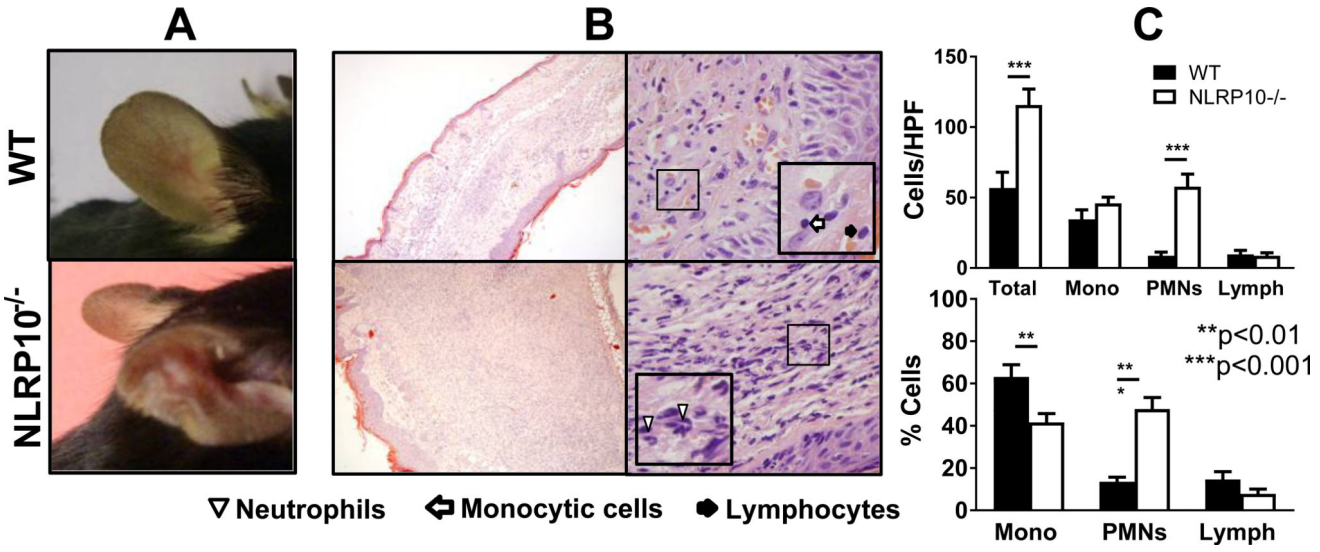

Figure 5. Late lesions: Late in *L. major* infection, ears of NLRP10$^{-/-}$ mice have increased tissue damage and enhanced infiltrating neutrophils compared to WT lesions

(A) Photographs of ear lesions from representative infected WT and NLRP10$^{-/-}$ mice after 70 days of *L. major* infection, and (B) histologic sections of H&E-stained, *L. major*-infected ear tissue on day 98 post-infection are shown. The lesions of WT (upper images) and NLRP10$^{-/-}$ (lower images) are shown at 100X (left images) or 1000X (right images) magnification (0.25 N.A. or 1.3 N.A., respectively), with insets illustrating specific cell types. (**C**) The absolute number and the percentage of cells per high power field (HPF), were determined microscopically on day 98 post inoculation with *L. major* . The results were compiled from 3 experiments with at least 2 injected ears per group and expressed as the mean ± SEM. Statistical analyses were done by one way ANOVA.

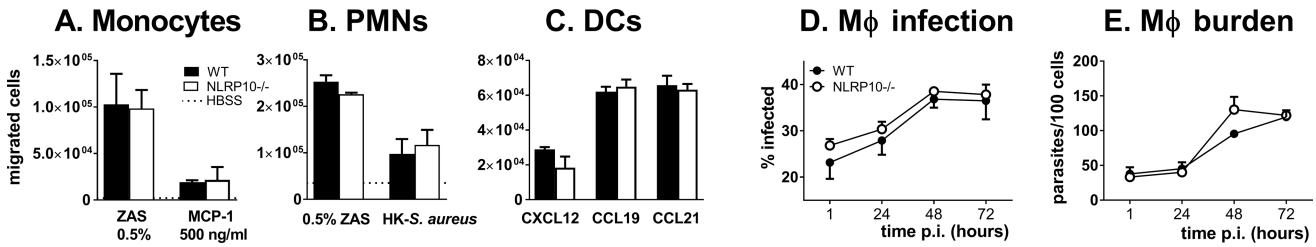

Figure 6. NLRP10$^{-/-}$ and WT myeloid cells have similar migration toward chemoattractants and leishmanicidal activity

(**A-C**) Transwell migration assays were performed with (**A**) PMNs, (**B**) monocytes, and (**C**) bone marrow-derived DCs. The WT and NLRP10$^{-/-}$ monocytes were isolated from bone marrow and analyzed in a transwell migration assay for their migration toward zymosan activated serum or MCP-1. (**B**) WT and NLRP10$^{-/-}$ PMNs were isolated from bone marrow and tested in a transwell assay for migration toward zymosan activated serum or heat-killed *S. aureus.* (**C**) WT or NLRP10$^{-/-}$ bone marrow-derived DCs were assayed in a transwell assay for their migration toward CCL12, CCL19, or CCL21. **D-E**) To test their intracellular survival, serum opsonized, metacyclic *L. major* WT Friedlin strain promastigotes were added to WT or NLRP10$^{-/-}$ BMDMs at a parasite to macrophage ratio of 5:1 . (**D**) The percent infection and (**E**) parasites/100 macrophages were quantified microscopically at the indicated times post infection. Results were compiled from 3 independent experiments, each with triplicate slides, and expressed as the mean ± SEM.

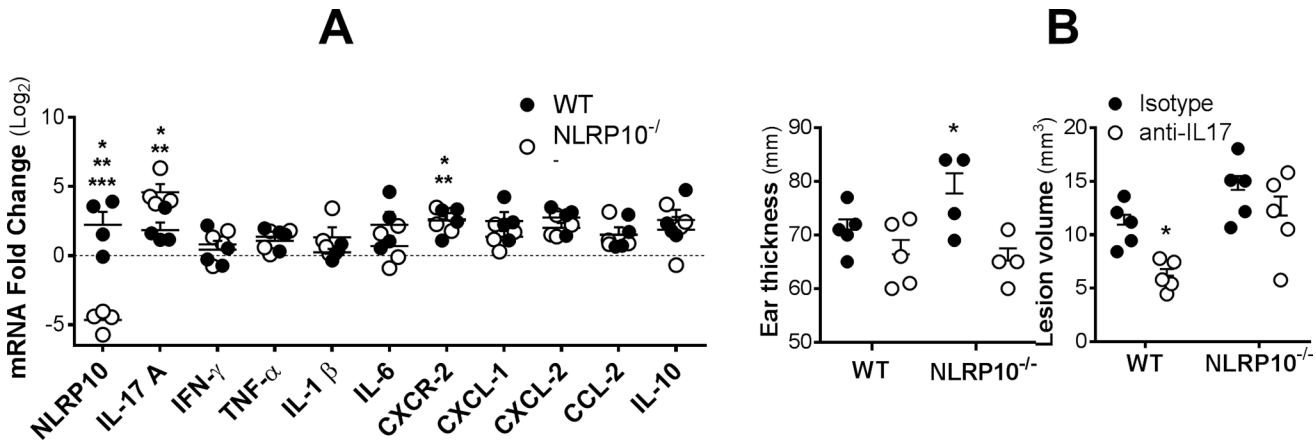

Figure 7. In situ gene expression in ears of infected WT or NLRP10$^{-/-}$ mice

Either wild type C57BL/6 or NLRP10$^{-/-}$DOC8$^{+/+}$ mice were infected intradermally in the ear with 5×10^5 *L. major* promastigotes. (A), RNA was extracted from ears of WT or NLRP10$^{-/-}$ mice after 4 weeks of infection. In situ gene expression was measured by multiplex RT-qPCR using the Fluidigm method. Fold change was calculated against GAPDH as an endogenous control, using the ΔΔCT method comparing infected WT (closed circles) or NLRP10$^{-/-}$ (open circles) mice compared to uninfected WT mice. Statistical analyses were performed by one-way ANOVA. Asterisks indicate *p<0.05 comparing mRNA abundance in infected NLRP10$^{-/-}$ versus infected WT mice, or **p<0.05 comparing infected versus uninfected mice of the same strain (p<0.05) for both WT and NLRP10$^{-/-}$ mice). *** Baseline NLRP10 expression also differed between uninfected WT and NLRP10−/− mice (p<0.0001), as expected. (B) Mice were treated with anti-IL-17 or isotype control antibody prior to infection and twice weekly thereafter. Shown are the ear thickness at 2 weeks (left), or the lesion volume after 4 weeks of infection, at which time ulceration had occurred. (two way ANOVA)

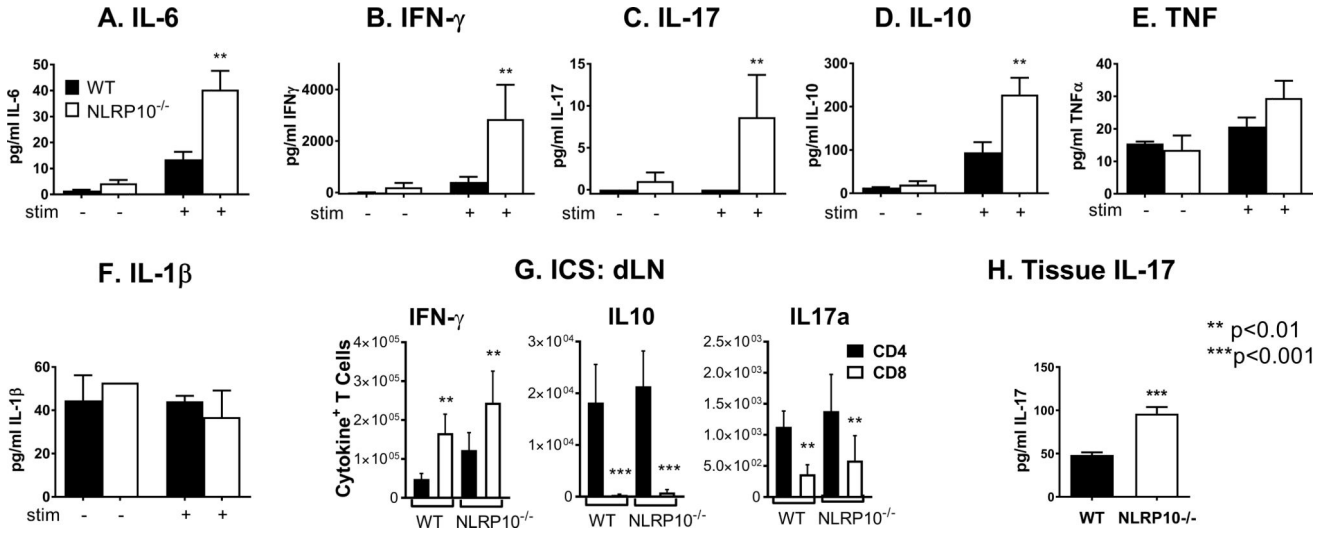

Figure 8. Cytokine responses during *L. major* infection in the absence of NLRP10

Mice were inoculated with 5×10^5 *L. major* stationary promastigotes intradermally in the ear pinna. (A-F) Two weeks post infection, cells from the draining lymph node were exposed to antigen (stim +) in the form of 1:5 promastigotes for 72 hours. Concentrations of the indicated cytokines in culture supernatants were measured using multiplex luminex assays. (G) Lymph nodes draining infected ears were harvested after 2 weeks of infection from WT or NLRP10$^{-/-}$ mice. Cytokine producing Thy1.2+ T cells were stained for surface CD4 or CD8, and for intracellular IFN-γ, IL-10 or IL-17a. Data show the mean ± SE cytokine positive cells from 3 experiments, each with 5 mice per group. Statistical analyses were done using ANOVA and Tukey's post-test. (H) IL-17 abundance in lysates from ears of infected mice was measured by ELISA after two weeks of infection. The results are compiled from 3 independent experiments, with a minimum of 5 mice per group and are expressed as the mean ± SEM. (* $p<0.05$, ** $p<0.01$, *** $p<0.001$, Wilcoxon rank sum test).

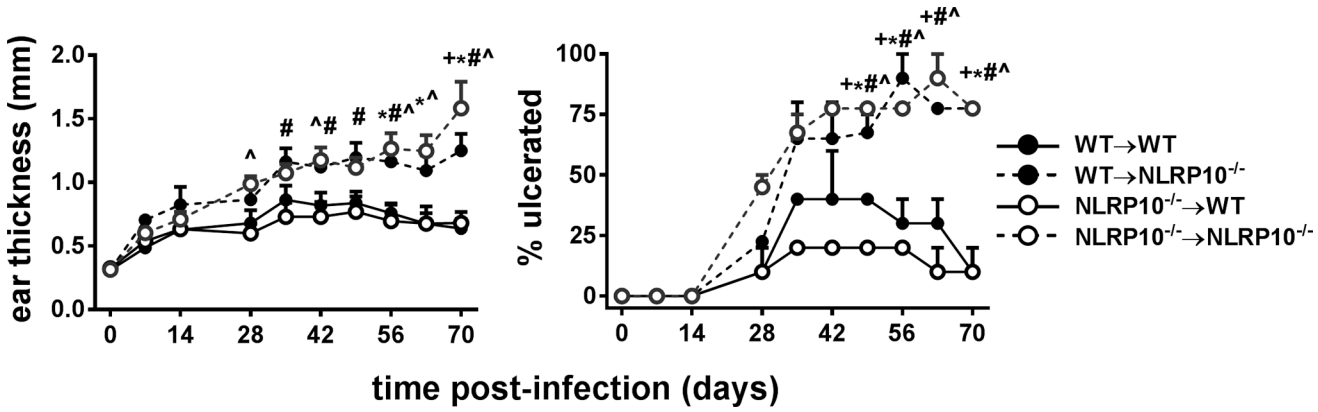

Figure 9. NLRP10 is required in the non-hematopoietic compartment for control of inflammation and ulceration

Bone marrow chimeras (donor hematopoietic cells->irradiated recipient; WT, wild type; 10, NLRP10$^{-/-}$) were inoculated with 5×10^5 *L. major* luciferase expressing stationary promastigotes intradermally in the ear pinna. (A) Lesion thickness and (B) ulceration were monitored by weekly caliper measurements of ear thickness and by visual inspection, respectively, for 10 weeks. Data show results in groups of 10 mice. Symbols indicate statistical comparisons between the groups that reached significance at the $p<0.05$ level (two way ANOVA). Groups with significant differences were: *WT→WT versus NLRP10$^{-/-}$→ NLRP10$^{-/-}$; +WT→WT versus WT→ NLRP10$^{-/-}$; ^ NLRP10$^{-/-}$→WT versus NLRP10$^{-/-}$→ NLRP10$^{-/-}$; # NLRP10$^{-/-}$→WT versus WT→NLRP10$^{-/-}$